# Structural differences in bacterial lipopolysaccharides determine atherosclerotic plaque progression by regulating the accumulation of neutrophils

Saito, Yoshihiro ; Yamashita, Tomoya ; Yoshida, Naofumi ; Emoto, Takuo ; Takeda, Shintaro ; Tabata, Tokiko ; Shinohara, Masakazu ; Kishino,…

(Citation)
Atherosclerosis,358:1-11

(Issue Date)
2022-10-01

(Resource Type)
journal article

(Version)
Accepted Manuscript



(URL)
https://hdl.handle.net/20.500.14094/0100476917

**Structural differences in bacterial lipopolysaccharides determine atherosclerotic plaque progression by regulating the accumulation of neutrophils**

**Running title:** Effect of differences in LPS on atherosclerosis

Yoshihiro Saito, MD[1]; Tomoya Yamashita, MD, PhD[1*]; Naofumi Yoshida, MD, PhD[1]; Takuo Emoto, MD, PhD[1]; Shintaro Takeda[1]; Tokiko Tabata, MD[1]; Masakazu Shinohara, MD, PhD[2,3]; Shigenobu Kishino, PhD[4]; Yuta Sugiyama, PhD[4]; Nahoko Kitamura[4]; Hiroyuki Yamamoto, MD, PhD[5]; Tomofumi Takaya, MD, PhD[5]; Jun Ogawa, PhD[4]; Ken-ichi Hirata, MD, PhD[1]

[1]Division of Cardiovascular Medicine, Department of Internal Medicine, Kobe University Graduate School of Medicine, Kobe, Japan

[2]Division of Epidemiology, Kobe University Graduate School of Medicine, Kobe, Japan

[3]The Integrated Center for Mass Spectrometry, Laboratory Medicine, Kobe University Graduate School of Medicine, Kobe, Japan

[4]Division of Applied Life Sciences, Graduate School of Agriculture, Kyoto University, Kyoto, Japan.

[5]Division of Cardiovascular Medicine, Hyogo Brain and Heart Center, Himeji, Japan

**Corresponding author:**

Tomoya Yamashita, MD, PhD

Division of Cardiovascular Medicine, Department of Internal Medicine

Kobe University Graduate School of Medicine

7-5-1 Kusunoki-cho, Chuo-ku, Kobe 6500017, Japan

Phone: +81-78-382-5111

Fax: +81-78-382-5859

E-mail: tomoya@med.kobe-u.ac.jp

**Final word count: 5983**words

**Figure 1-5, FigureS1-5, TableS1, S2**

**Abstract**

**Background and aims:** Gut microbial lipopolysaccharide (LPS) induces endotoxemia, an independent risk factor for cardiovascular disease (CVD). However, no studies have demonstrated how structural differences in the each bacterial LPS contribute to endotoxemia. Here, we investigated the effects of different acyl chains in the lipid A moiety of LPS on endotoxemia and the subsequent immune response and atherosclerotic plaque formation.

**Methods:** *Apoe*$^{-/-}$ mice were intraperitoneally administered 2 mg/kg of *Escherichia coli*-derived LPS (E. LPS, as a representative of hexa-acylated lipid A), *Bacteroides*-derived LPS (B. LPS, as a representative of penta- or tetra-acylated lipid A), or saline (control) once a week, six times. An immunohistological assessment was performed on the plaque sections.

**Results:** E. LPS administration induced endotoxemia, but B. LPS and saline did not. In E. LPS-treated mice, total plaque areas in the aortic root were significantly increased, and neutrophil accumulation and increased formation of neutrophil extracellular traps (NETs) were observed at the plaque lesions, but not in B. LPS-treated mice. A single dose of E. LPS significantly increased the accumulation of neutrophils in plaque lesions on day 3, and NET formation on day 7. E. LPS also increased interleukin-1 beta (IL-1β) production in plaque lesions on day 7. Furthermore, NET formation and IL-1β production were also observed in human coronary plaques.

**Conclusions:** We identified a previously unknown link between structural differences in LPS

and atherosclerosis. Lowering microbial LPS activity may reduce NET formation in plaques and prevent CVD progression.

**Clinical Trial Registration:** Unique identifier: UMIN 000040747

URL: https://upload.umin.ac.jp/cgi-open-bin/icdr_e/ctr_view.cgi?recptno=R000046521

## Introduction

Endotoxemia, characterized by high plasma lipopolysaccharide (LPS) activities, is strongly associated with cardiovascular disease (CVD) progression. Clinical studies have shown that high plasma LPS levels are an independent risk factor for CVD [1] by stimulating an innate immune response and producing pro-inflammatory cytokines via Toll-like receptor 4 (TLR4) signaling [2]. Furthermore, plasma LPS levels have been reported to be elevated in patients with ischemic stroke relative to those in controls and correlate with worsening disability [3, 4].

Since the translocation of gut microbial LPS induces endotoxemia, the gut microbiota and gut permeability play a key role in the pathophysiology underlying endotoxemia. Indeed, patients with type 2 diabetes show gut dysbiosis, and gut bacteria are detected in their blood [5]. In particular, a high-fat diet causes a chronic increase in plasma LPS activities, called metabolic endotoxemia [6]. An interventional study indicated that modifying the gut microbiota alleviates metabolic endotoxemia in patients with metabolic syndrome [7]. In heart failure patients, plasma LPS levels are elevated during acute edematous exacerbation, and enhanced diuretic administration can normalize LPS levels [8]. These findings suggest that the gut microbiota composition and intestinal permeability are the main determinant factors for metabolic endotoxemia.

The lipid A moiety of LPS is the main microbe-associated molecular pattern (MAMP) that acts on TLR4, and the number of acyl chains in lipid A is a key determinant of immune activation

by the LPS-TLR4 system. Interestingly, the penta- or tetra-acylated lipid A moiety of LPS derived from *Bacteroides* species (B. LPS) showed lower immunogenicity than the hexa-acylated lipid A of *E. coli* LPS (E. LPS), as we have previously reported [9]. Specifically, B. LPS mediated the production of relatively lower levels of pro-inflammatory cytokines than E. LPS *in vitro* and did not induce sepsis *in vivo* [9]. A recent study on endotoxemia and atherosclerosis suggests that neutrophils, especially NETs, exacerbate atherosclerosis by recruiting monocytes to the arterial wall [10]. However, no studies have demonstrated how structural differences in the lipid A moiety of each bacterial LPS contribute to endotoxemia and the subsequent immune response as well as atherosclerotic plaque formation.

To address this gap, we aimed to administer E. LPS and B. LPS to atherosclerotic mice to induce endotoxemia and examine the systemic and local immune responses and atherosclerotic plaque progression. The findings of this study might be valuable in clarifying whether the composition of gut microbiota is a target for regulating endotoxemia-related inflammatory diseases, including CVD.

## Materials and methods

### LPS extraction and lipid A isolation

LPS was purified using the hot phenol-water method as previously described by Yoshida et al. [9]. Lipid A isolation was performed as described by Sándor et al. with minor modification [11]. Briefly, lipid A was extracted from each LPS using mild-acid hydrolysis with 1 % (v/v) AcOH and shaking at 100 °C for 1 h, and the solution was lyophilized; 1 mL distilled water was then added, and the solution was centrifuged (8,000 × *g*, 4 °C, 10 min). The pellet was washed with distilled water four times. All lipid A samples were dissolved in methanol/trichloromethane (95:5, v/v), sonicated, and finally filtered via a 0.22-μm filter.

### Animal model

Apolipoprotein E–deficient mice (offspring of homozygous *Apoe*$^{-/-}$ mice, backcrossed onto the C57BL/6 background) were bred in a specific pathogen-free environment in the institute for Eexperimental Aanimals, at Kobe University. *Tlr4*$^{-/-}$ mice on a C57BL/6J background were purchased from Charles River Japan (Yokohama, Japan). They were allowed ad libitum access to water and a standard chow (CE-2, CLEA, Tokyo, Japan) and kept under a 12-h light-dark cycle. 8-week-old *Apoe*$^{-/-}$ female mice were fed a western diet (CE-2 82.7 %, cocoa butter 17 %, cholesterol 0.2 %, CLEA, Tokyo, Japan) for 6 weeks. *E. coli* LPS purified by phenol extraction (#L2630; Sigma-Aldrich) was used as E. LPS. Mice were injected intraperitoneally with 2

mg/kg of E. LPS or a total of 2 mg/kg B. LPS from *B. dorei* and *B. vulgatus*, one half of each in 200 µl of LPS-free water once a week. A total of 200 µl LPS-free water was used as a control. Three days after the last LPS administration, the mice were euthanized for analyses. In NETs inhibition model, 8 weeks-old *Apoe*$^{-/-}$ female mice were fed a western diet for 6 weeks. Mice were injected intraperitoneally with 2 mg/kg of E. LPS once a day, and 10 mg/kg DNase I (#D5025; Sigma-Aldrich) in 100 µl 0.9 % sodium chloride solution or as control 100 µl 0.9 % sodium chloride only five times weekly, and euthanized three days after the last LPS administration.

To investigate the morphological changes in atherosclerotic plaque after a single dose of LPS administration, 8-week-old *Apoe*-/- female mice were fed a western diet for 10 weeks, and the mice were injected intraperitoneally with 2 mg/kg of E. LPS or 2 mg/kg of B. LPS in 200 µL of LPS-free water three or seven days before euthanization. As a control, 200 µL of LPS-free water was administered three days before euthanization. In the experiment to confirm LPS in the plaque, mice were euthanized 24 hours after an intraperitoneal administration of 2 mg/kg of Alexa Fluor 594-conjugated *E. coli*-derived LPS (#L23353; Invitrogen). Anti-Ly6G (clone 1A8, #BE0075-1; Bio X Cell), anti-rat kappa immunoglobulin (clone MAR 18.5, #BE0122; Bio X Cell), and isotype controls (#BE0089 and #BE0085; Bio X Cell) were intraperitoneally injected starting the day before LPS administration to deplete neutrophils following the schemes and dosage described by Boivin et al. [12] and mice were euthanized seven days after

LPS administration. After euthanization, the aortae were rinsed by perfusion with phosphate-buffered saline from the left ventricle of the heart. Subsequently, the hearts and aortae were removed and fixed with 4 % paraformaldehyde at 4 °C overnight, and frozen sections of the aortic root were prepared and analyzed. This study was approved by the Animal Ethics Committee at Kobe University (P190706) and conducted following the guidelines for animal experiments at Kobe University School of Medicine.

**Atherosclerotic lesion assessment**

Samples were obtained from the proximal ascending aorta to the aortic sinus to analyze aortic root lesions. The samples were embedded in an optimal cutting temperature compound (#4583; Tissue-Tek Sakura Finetek, Tokyo, Japan). Six (for Figure1E, S1F) or seven (for Figure S2M) consecutive sections (10 μm in thickness) spanning 600 μm (for Figure1E, S1F) or 700 $\mu$m (for Figure S2M) of the aortic sinus from each mouse were stained with Oil Red O (#154-02072; Sigma-Aldrich) in 60 % isopropyl alcohol for 10 min, washed with water, and counterstained with Mayer's hematoxylin for lesion quantification. The stained sections were captured digitally using a microscope (#BZ-8000; Keyence, Osaka, Japan). For the quantitative analysis of the extent of atherosclerosis, the total lesion area was calculated for six separate sections obtained from each mouse using the ImageJ software, as previously described [13]. For immunofluorescence staining of the aortic root, adjacent sections were used. The tissue was

permeabilized with 0.2 % Triton X-100 in PBS for 10 min and blocked with 2 % goat or donkey serum at room temperature for 1 h and then incubated at 4 °C overnight with the primary antibodies diluted in blocking buffer: anti-CD68 (#137011; BioLegend), anti-mac2 (clone M3/38, # CED-CL8942LE; BIOZOL), anti-Ly6G (clone 1A8, #BD551461; BD Biosciences), anti-Histone H3 (citrulline R2 + R8 + R17) antibody (#ab5103; Abcam), and anti-IL-1β/IL-1F2 antibody (#AF-401-NA; R&D Systems). Slides were washed and incubated at room temperature for 2 h with the secondary antibodies: Alexa Fluor 647-conjugated goat anti-rabbit IgG (#A21244; Invitrogen) and Alexa Fluor 647-conjugated donkey anti-goat IgG (#ab150135; Abcam). The slides were then counterstained with DAPI (#422801; BioLegend). Finally, the slides were mounted in Dako fluorescence mounting medium (#S3023; Dako) and captured digitally using a fluorescence microscope (#BZ-8000; Keyence, Osaka, Japan). We evaluated CD68-positive or Ly6G-positive living cell counts co-stained with DAPI excluding the fractioned DAPI staining by setting the threshold of intensity of DAPI signals to exclude the fractioned nuclei. We used TUNEL Assay Kit (#48513; Cell Signaling Technology) in TUNEL staining according to the manufacturer's instructions. Images were analyzed using the BZ-X analyzer. We also analyzed en face atherosclerotic lesion size stained by Oil Red O in the lesser curvature of the ascending to arch aortae (between the aortic root and the left subclavian artery).

**Cell collection and flow cytometry**

For flow cytometry analysis, peripheral blood samples were collected from mice with heparin-coated capillary tubes. Erythrocytes were lysed by 1X RBC lysis buffer (BioLegend) for 10 min and the number of total blood cells was counted by diluting 1:20 with RBC lysis buffer. For the analysis of bone marrow hematopoietic cells, femurs were crushed with a mortar and pestle and filtered via a 40-μm nylon mesh. The spleens were homogenized and filtered using a 40-μm nylon mesh, and erythrocytes were lysed by 1X RBC lysis buffer. The antibodies used for the flow cytometry are listed in **Table S1**. Flow cytometry was performed by a LSR Fortessa cell analyzer (BD Biosciences) and the data were analyzed by FlowJo v10.7.1 (Tree Star, Inc.).

**Human samples**

We prospectively enrolled patients according to the AHA/ACC guidelines [14-16]. The participants provided oral and written informed consent, and the study was conducted according to the guidelines of the Declaration of Helsinki. This study was approved by the Ethics Committee of Kobe University (approval no. B200139) and registered with the UMIN Clinical Trials Registry (trial registration no. UMIN 000040747). Samples of coronary artery plaque were obtained following directional coronary atherectomy (DCA) performed on patients with the acute coronary syndrome (ACS) and were fixed in 4 % paraformaldehyde overnight. The sections were then embedded in paraffin. Subsequently, the sections were sliced

with a thickness of 4 μm, and stained with hematoxylin and eosin and Masson's trichrome. Immunohistochemistry was performed using anti-CD68 antibody (#M0876; Dako), followed by biotinylated secondary antibodies and streptavidin–horseradish peroxidase. For immunofluorescence staining, tissue sections were incubated at 4 °C overnight with anti-human myeloperoxidase (MPO) (#AF3667; R&D Systems), anti-histone H3 (citrulline R2 + R8 + R17) antibody (#ab5103; Abcam), and anti-human IL-1 β (#MAB601; R&D Systems) antibodies. The slides were washed and incubated with the following secondary antibodies: Alexa Fluor 568–conjugated donkey anti-goat (#ab175704; Abcam), Alexa Fluor 488–conjugated donkey anti-rabbit (#406416; BioLegend), and Alexa Fluor 647–conjugated donkey anti-mouse (#A-31571; Invitrogen). Finally, the slides were mounted and captured digitally using a fluorescence microscope.

**Statistical analysis**

Statistical analyses were performed using the GraphPad Prism version 8.3.1. The Shapiro–Wilk test was used to determine data normality. The results were presented as the mean ± SEM. For two-group comparison, the two-tailed Student's t-test was used for normally distributed data or the Mann–Whitney U test was used for non-normally distributed data. For multiple comparisons, one-way analysis of variance (ANOVA) with Tukey's post-hoc test was used for normally distributed data or Kruskal–Wallis test with Dunn's post-hoc test was used for non-

normally distributed data. Quantitative comparisons of each plaque area at six aortic root sections were performed with two-way ANOVA. Statistical significance was defined at $p < 0.05$.

## Results

### Effects of differences in E. LPS and B. LPS on plaque progression

We first isolated lipid A from E. LPS and B. LPS (*B. dorei* and *B. vulgatus* LPS) and analyzed the structure by liquid chromatography-tandem mass spectrometry (LC-MS/MS). We confirmed that the lipid A moiety isolated from E. LPS was hexa-acylated, whereas those from both B. LPS were tetra- and penta-acylated (**Figure 1A**). The E. LPS activity, measured via limulus amebocyte lysate (LAL) assay, was considerably higher than that of the LPS derived from B. LPS (**Figure S1A**); this was consistent with the findings of previous reports [9]. Next, we investigated the effects of structural differences in LPS on endotoxemia and observed a significant elevation in plasma LPS activity 24 h after intraperitoneal administration of 2 mg/kg of E. LPS; however, such an increase was not observed when the same dose of B. LPS was administered (**Figure 1B**). We performed experiments using a mouse model of atherosclerosis to determine the effect of repeated endotoxemia on the atherosclerotic plaque (**Figure 1C**). No death was observed in both groups and no significant differences were observed in body weight changes (**Figure S1B**), and total cholesterol levels in plasma were lower in the E. LPS-treated group than in the B. LPS-treated group; however, the triglyceride levels were not changed in the LPS-treated groups (**Figure S1C**). Mice with repeated endotoxemia induced by E. LPS showed a significant increase in the area of atherosclerotic plaque lesions, whereas those injected with B. LPS showed no changes

(**Figure 1D, E**). There were no differences in aortic arch plaque between each group (**Figure S1D, E**). The same repeated E. LPS administration in *TLR4*$^{-/-}$ *Apoe*$^{-/-}$ mice did not worsen the plaque burden (**Figure S1F**). This result supports that TLR4-mediated signaling from lipid A is critical for plaque exacerbation induced by endotoxemia.

**Immunological changes in plaques induced by structural differences in LPS**

Immunofluorescence staining was performed on aortic root sections to determine which immune cells showed increased numbers in the plaque lesions (**Figure 2A**). There were no significant changes in CD68 (macrophage marker)-positive area or cell counts in the LPS-treated groups (**Figure 2B**), and nor in samples stained with mac2 antibody. (**Figure S2B, C**). However, Ly6G (neutrophil marker)-positive area or cell counts significantly increased in the E. LPS-treated group (**Figure 2C**). The CD68-positive and Ly6G-positive areas per total plaque area did not change between 3 groups (**Figure S2A**). However, there was a positive correlation between the Ly6G positive area and total lesion plaque area (**Figure S2D**), suggesting that LPS with hexa-acylated lipid A may increase plaque formation by accumulating neutrophils rather than macrophages. Interestingly, more TUNEL-positive cells were found in the plaques of the E. LPS-treated group than control group in areas where Ly6G positive neutrophils were accumulated (**Figure S2E, F**). This finding suggests that E. LPS induces both apoptosis and NETs at the same sites in the atherosclerotic plaques, where neutrophils were

accumulated. We hypothesized that neutrophil infiltration induced by E. LPS was associated with plaque exacerbation, and then focused on the formation of neutrophil extracellular traps (NETs), which are involved in a mechanism underlying the promotion of atherosclerosis by neutrophils [17]. As shown in previous studies [18], citrullinated histone-3 (Cit-H3)-positive areas were identified in the Ly6G-positive area, indicating that NETs were formed in the plaque lesion (**Figure 2D**). Analysis of the total size of Cit-H3+ Ly6G+ areas in each group showed that NET formation was significantly increased in the E. LPS-treated group compared to that in the control and the B. LPS-treated groups, and the activity of the induction of NET formation, adjusted for the area of neutrophils, was also higher for E. LPS than for B. LPS (**Figure 2E, F**). We performed in vitro experiments to assess whether LPS stimulation directly induces NET formation via TLR4 on neutrophils. Isolated neutrophils from murine bone marrows did not show a significant increase in extracellular DNA after E. LPS or B. LPS stimulation in vitro (**Figure S2G, H**), suggesting that NET formation in plaque lesions caused by the interactions with other cells rather than the direct LPS stimulation. In aortic tissue with plaque lesions, we measured mRNA expression levels of representative chemokines involved in neutrophil recruitment and activation by real time PCR and found that *Ccl5* expression was significantly higher in the E. LPS treated-group than the B. LPS-treated or control groups (**Figure S2I**). Plasma CCL5 protein levels determined by ELISA were also higher in the E. LPS-treated group than the B. LPS-treated group (**Figure S2J**). CD68-positive, Ly6G-positive, Cit-H3+ Ly6G+

areas in the plaque lesions at aortic root from *Tlr4*$^{-/-}$ *Apoe*$^{-/-}$ mice after repeated LPS administration were not increased (**Figure S2K)**. We performed a NETs inhibition experiment by DNase I administration to confirm the effect of NETs on atherosclerotic plaque formation, but we did not observe a significant decrease in the total plaque areas in the DNase I-treated group (**Figure S2L, M**).

**Distinctive systemic immune response attributed to structural differences in LPS**

Blood, spleen, and bone marrow cells obtained after repeated LPS administration were analyzed by flow cytometry to confirm the systemic immune response to endotoxemia. No changes were observed in the counts of monocytes, T cells, and B cells in the blood, but the neutrophil count was significantly reduced in the E. LPS-treated group (**Figure 3A and Figure S3A**). In the spleen, a minor increase was observed in the neutrophils count in the E. LPS-treated group compared to that in the B. LPS-treated group; however, the difference was not significant (**Figure 3B and S3B**). In the bone marrow, both LPS groups showed an increase in cell numbers; however, only the E. LPS-treated mice showed a tendency of reduction in the number of mature neutrophils and a significant increase in the number of neutrophil progenitor cells (pre-neutrophils and immature neutrophils) (**Figure 3C, D**). We observed a reduced population of monocytes in bone marrow in the E. LPS-treated group, but no changes were observed in monocyte progenitor cells (**Figure S3C, D**). The percentage of CXCR2-negative

neutrophils in peripheral blood significantly increased the day after E. LPS administration and normalized on day 3, but these changes were not observed in the B. LPS-treated group (**FigureS3E, F, and G**), suggesting that E. LPS stimulation promotes emergency granulopoiesis and immature neutrophils are released from bone marrow. These results suggest that endotoxemia enhances the production of neutrophil progenitor cells and the release of neutrophils from bone marrow, leading to the migration of neutrophils from peripheral blood to tissues such as aortae.

**The course of NET formation and IL-1β production in plaque caused by a single LPS administration**

To investigate the causal relationship between neutrophil accumulation in the plaque and plaque exacerbation due to endotoxemia, we performed murine experiments with a single LPS administration (**Figure 4A**). First, to confirm whether the administered LPS was present in the plaque lesion, mice were euthanized 24 h after intraperitoneal administration of 2 mg/kg of *E. coli* derived LPS conjugated with Alexa Fluor 594 aortic root sections were observed. Conjugated E. LPS was observed on the plaque surface and between the plaque and vascular endothelium (**Figure 4B**). Second, the mice were euthanized on day 3 or day 7 after LPS (non-conjugated) administration, and the aortic root sections were analyzed via immunofluorescence staining. No significant changes were observed in the macrophage areas, but the neutrophil

areas increased on day 3 after E. LPS administration and then decreased on day 7 (**Figure 4C, D**). In the E. LPS-treated group, the formation of NETs increased on day 7 and was delayed after the increase in the neutrophil area (**Figure 4C, D**). In addition, the IL-1β-positive area significantly increased in the E. LPS-treated group on day 7 when the formation of NETs increased (**Figure 4E, F**). Immunofluorescence staining revealed that IL-1β was more abundant in the regions around neutrophils and NETs (**Figure 4C, E**). There were no significant changes in the areas of macrophages, neutrophils, NETs formation, and IL-1β production in plaque lesions in the B. LPS-treated group (**Figure 4D, F, and Figure S4A, B**). Single LPS administration did not affect total plaque areas on day 7. (**FigureS4C**). In the neutrophil depletion experiment (**Figure S4D**), anti-Ly6G treatment decreased the number of neutrophils in the blood and Ly6G-positive areas in the aortic root plaque lesions (**Figure S4E, F**). There were no differences in total plaque area on day 7 after anti-Ly6G treatment (**Figure S4H**), but a pattern of slightly decreased IL-1β-positive areas relative to CD68-positive areas (**Figure S4G**). These data indicated that neutrophil accumulation in the plaque lesion might be involved in activation of macrophages and production of inflammatory cytokines.

**Immunohistochemical analysis of human coronary artery plaque**

Immunostaining was performed with plaque lesions from patients with ACS who underwent DCA to elucidate whether neutrophil accumulation, NET formation, and IL-1β production

occur in human coronary plaques. In human coronary plaques, neutrophils, characterized by MPO-positive cells, were accumulated in macrophage-rich areas, and Cit-H3 positive cells were also observed in the same areas (**Figure 5A, B**). Furthermore, we observed an IL-1β-positive area at the near site of NET formation (**Figure 5C, D**). These results indicate that NET formation and IL-1β production also occur in human atherosclerotic plaque lesions, suggesting that neutrophil migration by endotoxemia may be involved in CVD progression.

## Discussion

In this study, we clarified that structural differences in the lipid A moiety of each bacterial LPS contribute to endotoxemia and the subsequent immune response and atherosclerotic plaque formation. The primary findings are listed as follows: 1) *Escherichia coli* LPS (hexa-acylated lipid A) strongly induced endotoxemia, whereas LPS of *Bacteroides* species (penta- or tetra-acylated lipid A) did not; 2) Endotoxemia induced the accumulation of neutrophils in atherosclerotic plaque lesions and subsequent NET formation and IL-1β production; 3) NET formation and IL-1β production were observed in human coronary artery plaques. Overall, our findings provide insights into the roles of the gut microbial LPS structure in endotoxemia and CVD progression.

The composition of the gut microbiota and intestinal permeability are considered crucial for developing endotoxemia. Our results provide insights into the role of lipid A, a ligand for TLR4, and a potent determinant of immune activation, as it plays a pivotal role in endotoxemia and CVD. TLR4 forms the TLR4-MD-2 complex, and lipid A activates TLR4 by binding to MD-2. Compared to the hexa-acylated lipid A, the penta-acylated lipid A binds with a lower affinity to MD-2, and different charge distributions and orientations affect the binding ability [19]. Interestingly, acyloxyacyl hydrolase (AOAH), which inactivates LPS by cleaving the secondary fatty acyl chain of lipid A, has been demonstrated to reduce carotid plaque lesions in mice after LPS exposure [20]. This finding strongly supports our hypothesis that structural

differences in LPS determine CVD progression. Among many species of the gut microbiota, we demonstrated that LPS from *B. dorei* and *B. vulgatus*, which is composed of penta- or tetra-acylated lipid A, is significantly less immunogenic than E. LPS, which consists of hexa-acylated lipid A, as assessed via an in vitro stimulation assay and in vivo sepsis model [9]. We also demonstrate that the abundance of *B. dorei* and *B. vulgatus* is significantly reduced while that of *E. coli* tends to increase in the gut of patients with coronary artery disease [21]. Another clinical study performed in China with many patients also supports our data, showing a relative decrease in *Bacteroides* species and enrichment of *E. coli* in patients with atherosclerotic CVD [22]. Moreover, we have previously demonstrated a significant negative correlation between the abundance of *Bacteroides* and the LPS activity in human feces [9]. These findings indicate that high LPS immunogenicity of the gut microbiota may be associated with CVD progression, and the current results support the hypothesis that increased abundance of *B. dorei* and *B. vulgatus* may prevent endotoxemia and subsequent CVD.

Atherosclerosis is considered to be a chronic inflammatory disease involving many different cells, and previous studies have focused on the enhanced inflammatory response mediated by macrophages. Specifically, monocytes that accumulate on activated endothelial cells differentiate into macrophages, which are activated by the binding of MAMPs and damage-associated molecular patterns (DAMPs), and release inflammatory molecules such as pro-inflammatory cytokines, chemokines, and oxygen radicals. In fact, E. LPS (major MAMP) was

localized in the human carotid plaque [23], which is consistent with the hypothesis that upon entering the bloodstream, bacterial LPS induces inflammation by depositing on plaque lesions. This study showed that the administered LPS adhered to the plaque lesions on the following day. Several studies have reported that inflammatory immune responses induced by LPS injection in mice exacerbate atherosclerosis [24-26], and a significantly low dose of LPS can also exacerbate atherosclerosis [27]. However, the effect of LPS with penta- or tetra-acylated lipid A on atherosclerosis was not elucidated. In this study, administration of B. LPS did not induce endotoxemia and did not significantly worsen atherosclerosis. Because E.LPS did not affect enlargement of plaque area in the lesser curvature of the ascending to arch aortae, but severely affected plaque thickness in the aortic root section, we focused on aortic roots to evaluated the effect of E.LPS and B.LPS in this manuscript. Unexpectedly, there was no difference in macrophage accumulation between the LPS-treated and control groups, but endotoxemia induced by E. LPS significantly increased the accumulation of neutrophils in the plaque. Neutrophils are crucial for atherogenesis and arterial wall inflammation [28]. The present study showed an increase of protein levels of CCL5 in plasma and mRNA expression levels of *Ccl5* in aorta. The stimulation of neutrophils with CCL5 did not induce NET formation [29], suggesting that other chemokines and cellular signals may be involved in the NETs formation. In addition, increased neutrophil accumulation and NETs formation after LPS administration was canceled in *Tlr4*$^{-/-}$ *Apoe*$^{-/-}$ mice. Although we did not clarify the source of CCL5, it has been reported to

be secreted by many different cell types, such as endothelial cells, smooth muscle cells, macrophages, and platelets [30-33]. One of the studies demonstrated that platelet-derived CCL5 promotes arterial neutrophil recruitment [33]. Another study showed that LPS stimulation via platelet TLR4 induce platelet-neutrophil binding and neutrophil degranulation, resulting NET formation [34]. These data suggest that E. LPS stimulated CCL5 expression from platelets, endothelial cells or macrophages to induce the recruitment of neutrophils and NET formation through TLR4. In neutrophils of plaques, citrullination of histone tails, decondensation of chromatin, and disruption of the nuclear membrane occur, and the granular contents are released with the nuclear material [17]. NETs formed in these processes activate macrophages to produce inflammatory cytokines [18]. Our time-series analyses revealed the dynamic immune responses in atherosclerotic plaque following endotoxemia. The percentage of CXCR2-negative neutrophils in the peripheral blood was markedly increased the day after E. LPS administration and normalized on day 3. This result is consistent with the study demonstrating that E.LPS treatment lowered CXCR2 expression on neutrophils [35]. The increased number of neutrophil progenitor cells in the bone marrow also suggests that E. LPS stimulation may promote emergency hematopoiesis and release immature neutrophils into the blood stream. Neutrophil accumulation in plaque lesions was observed 3 days after administering a single dose of E. LPS, followed by subsequent NET formation and IL-1β production on day 7. These results are consistent with reports stating that NETs can activate macrophages to promote

cytokine production, and explain why E. LPS treatment did not change macrophage accumulation but exacerbated plaque. Furthermore, our study showed that this neutrophil accumulation and NETs formation by endotoxemia were not observed within a few hours but observed after a relatively long time (several days). NETs inhibition experiment by DNase I administration could not significantly suppress E. LPS induced plaque progression. The limitations of this experiment were that the influence of substances in neutrophils other than DNA, such as neutrophil elastase and chemotactic granule proteins like cathelicidin, could not be excluded. Further, LPS stimulated neutrophils directly and strongly; hence, the effect of DNase I could not be confirmed. In the neutrophil depletion experiment, anti-Ly6G treatment did not significantly reduce the IL-1β positive area. However, the effect of NETs could not be eliminated in this model because blood neutrophils were not removed on day 7; therefore, further studies are needed to understand the impact of NET formation by endotoxemia on plaque progression. Finally, NET formation and production of IL-1β were observed in human coronary plaques from the patients with ACS obtained by DCA. NET-derived H4 has been shown to bind to and lyse smooth muscle cells, accelerating plaque destabilization in mice [36]. A human study has shown that serum endotoxin levels in patients with end stage kidney disease with ACS was significantly higher than that without ACS [37]. Several human studies have reported plasma markers of NETs, such as dsDNA and nucleosome were higher in patients with ACS than those with stable angina pectoris and control group [38, 39]. Other human studies in

patients with ST-elevation myocardial infarction have shown that MPO, dsDNA and Cit-H3 levels were higher at the culprit lesion site than at the femoral site [40, 41]. Inhibition of endotoxemia and NET formation may contribute to the prevention of plaque exacerbation and the reduction of ACS events.

This previously unknown association between the LPS structure and endotoxemia and subsequent atherosclerotic plaque progression is the novelty of the present study. From a clinical perspective, given that gut microbial LPS is associated with the progression of not only CVD but also many other diseases, our findings may pave the way for future research on gut microbial LPS as a novel and attractive therapeutic strategy to suppress the inflammatory response and could contribute to the development of treatments for many patients. We have previously demonstrated that *Bacteroides*-based probiotics or resistant starch increase the abundance of *Bacteroides* in a gut model [9, 42], and are investigating their clinical applications.

In summary, we demonstrated that B. LPS, unlike E. LPS, does not induce endotoxemia and does not promote atherosclerosis (**Figure S5**). Clinically, intervention on gut microbial composition to enrich the abundance of *Bacteroides* may prevent the progression of endotoxemia and consequent CVD.

## Conflict of interest

The authors have no conflicts of interest directly relevant to the content of this article.

## Author contributions

Y. Saito, T. Yamashita (T.Y.), N. Yoshida (N. Y.), T. Emoto (T. E), M. Shinohara (M. S.), H. Yamamoto, T. Takaya, J. Ogawa (J. O.), and K. Hirata (K. H.) were involved in study conception and design. Y. Saito, T. Y., N. Y., T. E, S. Takeda, T. Tabata, M. S., S. Kishino, Y. Sugiyama, N. Kitamura, J. O., and K. H. were involved in analysis and interpretation of data. All authors critically revised the report, commented on drafts of the manuscript, and approved the final report.

## Acknowledgments

We thank Ryohei Shinohara, Hitomi Nakashima, Dr. Satoshi Uragami, and Dr. Jun Inoue for their excellent technical support. This work was supported by PRIME from the Japan Agency for Medical Research and Development (grant number 18069370 to T. Yamashita); the Japan Society for the Promotion of Science KAKENHI (grant number 19K23944 to N.Yoshida.; 19H03653 and 20K21603 to T. Y; and 20H03676 to K.Hirata.); and grants for Basic Research of the Japanese Circulation Society (to N.Y.).

## References


[1] Wiedermann, CJ, Kiechl, S, Dunzendorfer, S, et al., Association of endotoxemia with carotid atherosclerosis and cardiovascular disease: prospective results from the Bruneck Study, J Am Coll Cardiol, 1999;34:1975-1981.

[2] de Kleijn, D and Pasterkamp, G, Toll-like receptors in cardiovascular diseases, Cardiovasc Res, 2003;60:58-67.

[3] Klimiec, E, Pera, J, Chrzanowska-Wasko, J, et al., Plasma endotoxin activity rises during ischemic stroke and is associated with worse short-term outcome, Journal of neuroimmunology, 2016;297:76-80.

[4] Hakoupian, M, Ferino, E, Jickling, GC, et al., Bacterial lipopolysaccharide is associated with stroke, Scientific reports, 2021;11:6570.

[5] Sato, J, Kanazawa, A, Ikeda, F, et al., Gut dysbiosis and detection of "live gut bacteria" in blood of Japanese patients with type 2 diabetes, Diabetes care, 2014;37:2343-2350.

[6] Cani, PD, Amar, J, Iglesias, MA, et al., Metabolic endotoxemia initiates obesity and insulin resistance, Diabetes, 2007;56:1761-1772.

[7] Guevara-Cruz, M, Flores-López, AG, Aguilar-López, M, et al., Improvement of Lipoprotein Profile and Metabolic Endotoxemia by a Lifestyle Intervention That Modifies the Gut Microbiota in Subjects With Metabolic Syndrome, Journal of the American Heart Association, 2019;8:e012401.

[8] Niebauer, J, Volk, HD, Kemp, M, et al., Endotoxin and immune activation in chronic heart failure: a prospective cohort study, Lancet (London, England), 1999;353:1838-1842.

[9] Yoshida, N, Yamashita, T, Kishino, S, et al., A possible beneficial effect of Bacteroides on faecal lipopolysaccharide activity and cardiovascular diseases, Scientific reports, 2020;10:13009.

[10] Schumski, A, Ortega-Gómez, A, Wichapong, K, et al., Endotoxinemia Accelerates Atherosclerosis Through Electrostatic Charge-Mediated Monocyte Adhesion, Circulation, 2021;143:254-266.

[11] Sándor, V, Dörnyei, Á, Makszin, L, et al., Characterization of complex, heterogeneous lipid A samples using HPLC-MS/MS technique I. Overall analysis with respect to acylation, phosphorylation and isobaric distribution, Journal of mass spectrometry : JMS, 2016;51:1043-1063.

[12] Boivin, G, Faget, J, Ancey, PB, et al., Durable and controlled depletion of neutrophils in mice, Nature communications, 2020;11:2762.

[13] Sasaki, N, Yamashita, T, Takeda, M, et al., Oral anti-CD3 antibody treatment induces regulatory T cells and inhibits the development of atherosclerosis in mice, Circulation, 2009;120:1996-2005.

[14] Levine, GN, Bates, ER, Blankenship, JC, et al., 2011 ACCF/AHA/SCAI Guideline for Percutaneous Coronary Intervention: a report of the American College of Cardiology Foundation/American Heart Association Task Force on Practice Guidelines and the Society for Cardiovascular Angiography and Interventions, Circulation, 2011;124:e574-651.

[15] Amsterdam, EA, Wenger, NK, Brindis, RG, et al., 2014 AHA/ACC guideline for the management of patients with non-ST-elevation acute coronary syndromes: a report of the American College of Cardiology/American Heart Association Task Force on Practice Guidelines, Circulation, 2014;130:e344-426.
[16] Levine, GN, Bates, ER, Blankenship, JC, et al., 2015 ACC/AHA/SCAI Focused Update on Primary Percutaneous Coronary Intervention for Patients With ST-Elevation Myocardial Infarction: An Update of the 2011 ACCF/AHA/SCAI Guideline for Percutaneous Coronary Intervention and the 2013 ACCF/AHA Guideline for the Management of ST-Elevation Myocardial Infarction: A Report of the American College of Cardiology/American Heart Association Task Force on Clinical Practice Guidelines and the Society for Cardiovascular Angiography and Interventions, Circulation, 2016;133:1135-1147.
[17] Pérez-Olivares, L and Soehnlein, O, Contemporary Lifestyle and Neutrophil Extracellular Traps: An Emerging Link in Atherosclerosis Disease, Cells, 2021;10.
[18] Warnatsch, A, Ioannou, M, Wang, Q, et al., Inflammation. Neutrophil extracellular traps license macrophages for cytokine production in atherosclerosis, Science (New York, N.Y.), 2015;349:316-320.
[19] Ohto, U, Fukase, K, Miyake, K, et al., Structural basis of species-specific endotoxin sensing by innate immune receptor TLR4/MD-2, Proceedings of the National Academy of Sciences of the United States of America, 2012;109:7421-7426.
[20] Feng, J, Jiang, W, Cheng, X, et al., A host lipase prevents lipopolysaccharide-induced foam cell formation, iScience, 2021;24:103004.
[21] Yoshida, N, Emoto, T, Yamashita, T, et al., Bacteroides vulgatus and Bacteroides dorei Reduce Gut Microbial Lipopolysaccharide Production and Inhibit Atherosclerosis, Circulation, 2018;138:2486-2498.
[22] Jie, Z, Xia, H, Zhong, SL, et al., The gut microbiome in atherosclerotic cardiovascular disease, Nature communications, 2017;8:845.
[23] Carnevale, R, Nocella, C, Petrozza, V, et al., Localization of lipopolysaccharide from Escherichia Coli into human atherosclerotic plaque, Scientific reports, 2018;8:3598.
[24] Ostos, MA, Recalde, D, Zakin, MM, et al., Implication of natural killer T cells in atherosclerosis development during a LPS-induced chronic inflammation, FEBS letters, 2002;519:23-29.
[25] Westerterp, M, Berbée, JF, Pires, NM, et al., Apolipoprotein C-I is crucially involved in lipopolysaccharide-induced atherosclerosis development in apolipoprotein E-knockout mice, Circulation, 2007;116:2173-2181.
[26] Cuaz-Pérolin, C, Billiet, L, Baugé, E, et al., Antiinflammatory and antiatherogenic effects of the NF-kappaB inhibitor acetyl-11-keto-beta-boswellic acid in LPS-challenged ApoE-/- mice, Arteriosclerosis, thrombosis, and vascular biology, 2008;28:272-277.
[27] Geng, S, Chen, K, Yuan, R, et al., The persistence of low-grade inflammatory monocytes

contributes to aggravated atherosclerosis, Nature communications, 2016;7:13436.
[28] Döring, Y, Drechsler, M, Soehnlein, O, et al., Neutrophils in atherosclerosis: from mice to man, Arteriosclerosis, thrombosis, and vascular biology, 2015;35:288-295.
[29] Rossaint, J, Herter, JM, Van Aken, H, et al., Synchronized integrin engagement and chemokine activation is crucial in neutrophil extracellular trap-mediated sterile inflammation, Blood, 2014;123:2573-2584.
[30] Pattison, JM, Nelson, PJ, Huie, P, et al., RANTES chemokine expression in transplant-associated accelerated atherosclerosis, The Journal of heart and lung transplantation : the official publication of the International Society for Heart Transplantation, 1996;15:1194-1199.
[31] Hayes, IM, Jordan, NJ, Towers, S, et al., Human vascular smooth muscle cells express receptors for CC chemokines, Arteriosclerosis, thrombosis, and vascular biology, 1998;18:397-403.
[32] Schober, A, Manka, D, von Hundelshausen, P, et al., Deposition of platelet RANTES triggering monocyte recruitment requires P-selectin and is involved in neointima formation after arterial injury, Circulation, 2002;106:1523-1529.
[33] Drechsler, M, Megens, RT, van Zandvoort, M, et al., Hyperlipidemia-triggered neutrophilia promotes early atherosclerosis, Circulation, 2010;122:1837-1845.
[34] Clark, SR, Ma, AC, Tavener, SA, et al., Platelet TLR4 activates neutrophil extracellular traps to ensnare bacteria in septic blood, Nature medicine, 2007;13:463-469.
[35] Alves-Filho, JC, Sônego, F, Souto, FO, et al., Interleukin-33 attenuates sepsis by enhancing neutrophil influx to the site of infection, Nature medicine, 2010;16:708-712.
[36] Silvestre-Roig, C, Braster, Q, Wichapong, K, et al., Externalized histone H4 orchestrates chronic inflammation by inducing lytic cell death, Nature, 2019;569:236-240.
[37] Hsu, CC, Wei, TS, Huang, CC, et al., Endotoxemia is associated with acute coronary syndrome in patients with end stage kidney disease, BMC nephrology, 2017;18:235.
[38] Cui, M, Fan, M, Jing, R, et al., Cell-Free circulating DNA: a new biomarker for the acute coronary syndrome, Cardiology, 2013;124:76-84.
[39] Helseth, R, Solheim, S, Arnesen, H, et al., The Time Course of Markers of Neutrophil Extracellular Traps in Patients Undergoing Revascularisation for Acute Myocardial Infarction or Stable Angina Pectoris, Mediators of inflammation, 2016;2016:2182358.
[40] Mangold, A, Alias, S, Scherz, T, et al., Coronary neutrophil extracellular trap burden and deoxyribonuclease activity in ST-elevation acute coronary syndrome are predictors of ST-segment resolution and infarct size, Circulation research, 2015;116:1182-1192.
[41] Hofbauer, TM, Mangold, A, Scherz, T, et al., Neutrophil extracellular traps and fibrocytes in ST-segment elevation myocardial infarction, Basic research in cardiology, 2019;114:33.
[42] Yoshida, N, Sasaki, K, Sasaki, D, et al., Effect of Resistant Starch on the Gut Microbiota and Its Metabolites in Patients with Coronary Artery Disease, Journal of atherosclerosis and thrombosis, 2019;26:705-719.

**Keywords**

lipopolysaccharide, *Bacteroides,* endotoxemia, atherosclerosis, lipid A, neutrophil extracellular traps, IL-1β

**Abbreviations**

AOAH, acyloxyacyl hydrolase

ApoE, apolipoprotein E

Cit-H3, citrullinated histone 3

CAD, coronary artery disease

CVD, cardiovascular disease

DAMPs, damage-associated molecular patterns

DCA, directional coronary atherectomy

EU, endotoxin unit

IL-1β, interleukin-1beta

LPS, lipopolysaccharide

MAMP: microbe-associated molecular pattern

MPO, myeloperoxidase

NETs, neutrophil extracellular traps

TLR4, Toll-like receptor 4

**Figure legends**

**Figure 1. Structural differences in LPS determine atherosclerotic progression in a murine model.**

(A) Representative predicted structures and LC-MS/MS analysis of lipid A isolated from *E. coli*, *Bacteroides dorei*, and *Bacteroides vulgatus* LPS. We identified hexa-acylated structures from *E. coli* lipid A, and both penta- and tetra-acylated structures from *B. dorei* and *B. vulgatus* lipid A. (B) Plasma LPS activity of *Apoe*$^{-/-}$ mice that were administered 2 mg/kg of E. LPS, B. LPS, and LPS-free water. The blood was collected 24 h after LPS injection. (C) Experimental design for a murine model with repeated LPS administration. Female *Apoe*$^{-/-}$ mice were fed a western diet for six weeks with the administration of 2 mg/kg of E. LPS, B. LPS, or saline (control) intraperitoneally once a week for a total of six times. The mice were euthanized three days after the last LPS administration. (D) Representative microscopic images of Oil Red O staining of the area of atherosclerotic lesions in the aortic root derived from mice. Scale bars, 200 μm. (E) Quantitative analysis of each plaque area at six sections from the aortic root (left panel); the total plaque areas calculated from the area under the curve (AUC) shown in the left panel (right panel) (13 to 15 mice per group pooled from two independent experiments). Data are represented as mean ± SEM. Statistical analysis was performed using one-way ANOVA, followed by Tukey's post-hoc test for multiple comparisons (B, right panel of E), two-way ANOVA, followed by Dunnett's multiple comparison test, compared to the control. (left panel

of E): $^{**}p < 0.01$, $^{***}p < 0.001$. EU indicates endotoxin unit.

**Figure 2. *E. coli* LPS demonstrates a high ability to induce NET formation in plaque lesions.**

(A) Representative immunofluorescence microscopy images of aortic root from *Apoe*$^{-/-}$ mice intraperitoneally administered E. LPS or B. LPS or saline (control) once a week, six times. The mice were euthanized three days after the last LPS administration, and aortic root sections were stained with the macrophage marker CD68 (green), the neutrophil marker Ly6G (red), and DNA (DAPI, blue). Scale bars, 200 μm. (B, C) Quantitative analysis of CD68-positive area and cell counts (B) and Ly6G-positive area and cell counts (C) (13 to 15 mice per group pooled from two independent experiments). (D) Representative confocal immunofluorescence microscopy image of the aortic root section stained with Ly6G (red), the neutrophils extracellular trap marker citrullinated histone 3 (Cit-H3, cyan), and DNA (DAPI, blue). Scale bars, 50 μm. (E) Representative immunofluorescence microscopy image of the aortic root section stained with Cit-H3 (cyan). Scale bars, 200 μm. (F) Quantitation of cit-H3 positive areas of the aortic root plaque (top panel) and the cit-H3 positive area relative to the Ly6G-positive area (bottom panel) (13 to 15 mice per group pooled from two independent experiments). Data are represented as mean ± SEM. Statistical analysis was performed using one-way ANOVA, followed by Tukey's post-hoc test for multiple comparisons: $^{*}p < 0.05$, $^{**}p$

< 0.01; n.s., not significant.

**Figure 3. Stimulation with *E. coli* LPS increases the number of neutrophil progenitor cells in the bone marrow.**

(A) The numbers of total cells, monocytes, and neutrophils in the blood circulation of *Apoe*$^{-/-}$ mice intraperitoneally administered 2 mg/kg E. LPS, B. LPS, or saline (control) once a week, six times. Mice were euthanized three days after the last LPS administration, and samples were collected (11 or 12 mice per group pooled from two independent experiments). (B) Number of total cells, monocytes, and neutrophils in the spleen, as observed in two independent experiments (14 to 17 mice per group). (C) Flow cytometry gating strategy used to identify mature neutrophils, immature neutrophils, and pre-neutrophils in the bone marrow. (D) Number of total cells, mature neutrophils, immature neutrophils, and pre-neutrophils in the bone marrow, as observed in two independent experiments (6 or 9 mice per group). Data are represented as mean ± SEM. Statistical analysis was performed using one-way ANOVA, followed by Tukey's post-hoc test for multiple comparisons: *$p < 0.05$, **$p < 0.01$, ***$p < 0.001$.

**Figure 4. Endotoxemia induces neutrophil accumulation and subsequent NET formation in plaque lesions.**

(A) Experimental design for the murine model of single LPS administration. Female *Apoe*$^{-/-}$ mice were fed a western diet for 10 weeks and received 2 mg/kg of E. LPS, B. LPS, or saline (control) was intraperitoneally administered once three or seven days before euthanization. (B) Representative immunofluorescence microscopy images of aortic root sections from an *Apoe*$^{-/-}$ mouse administered Alexa Fluor 594 conjugated LPS (yellow). Aortic root sample was collected 24 h after LPS injection. Scale bars, 200 μm. (C) Representative immunofluorescence microscopy images of aortic root sections from the E. LPS-treated mice stained with the macrophage marker CD68 (green), the neutrophil marker Ly6G (red), the NET marker Cit-H3 (cyan), and DNA (DAPI, blue). Scale bars, 200 μm. (D) Quantitative analysis of CD68, Ly6G, Cit-H3-positive areas observed in two independent experiments (5 or 8 mice per group). (E) Representative immunofluorescence microscopic images of aortic root sections stained with IL-1β antibody (yellow). Scale bars, 200 μm. (F) Quantitative analysis of IL-1β-positive area was observed in two independent experiments (5 or 8 mice per group). Data are represented as mean ± SEM. Statistical analysis was performed using one-way ANOVA, followed by Tukey's post-hoc test for multiple comparisons: $*p < 0.05$, $**p < 0.01$, $***p < 0.001$; ns, not significant.

**Figure 5. NET formation and IL-1β production are observed in human coronary plaques.**

(A) Microscopic images of coronary artery plaque sections stained with hematoxylin and eosin (HE) (a), Masson's trichrome (b), CD68 (c), and myeloperoxidase (MPO) (red), citrullinated

histone 3 (Cit-H3, cyan), and DNA (DAPI, blue) (d); (b, c, d) close-up of the boxed area of (a). Scale bars, 100 μm. (B) High magnification images of the boxed area of Figure5A(d). Scale bars, 50 μm. (C) Immunofluorescence microscopic images of coronary artery plaque sections stained with MPO (red), citrullinated histone 3 (Cit-H3, cyan), IL-1β (yellow), and DNA (DAPI, blue). Scale bars, 100 μm. (D) High magnification images of the boxed area of Figure5C. Scale bars, 50 μm.

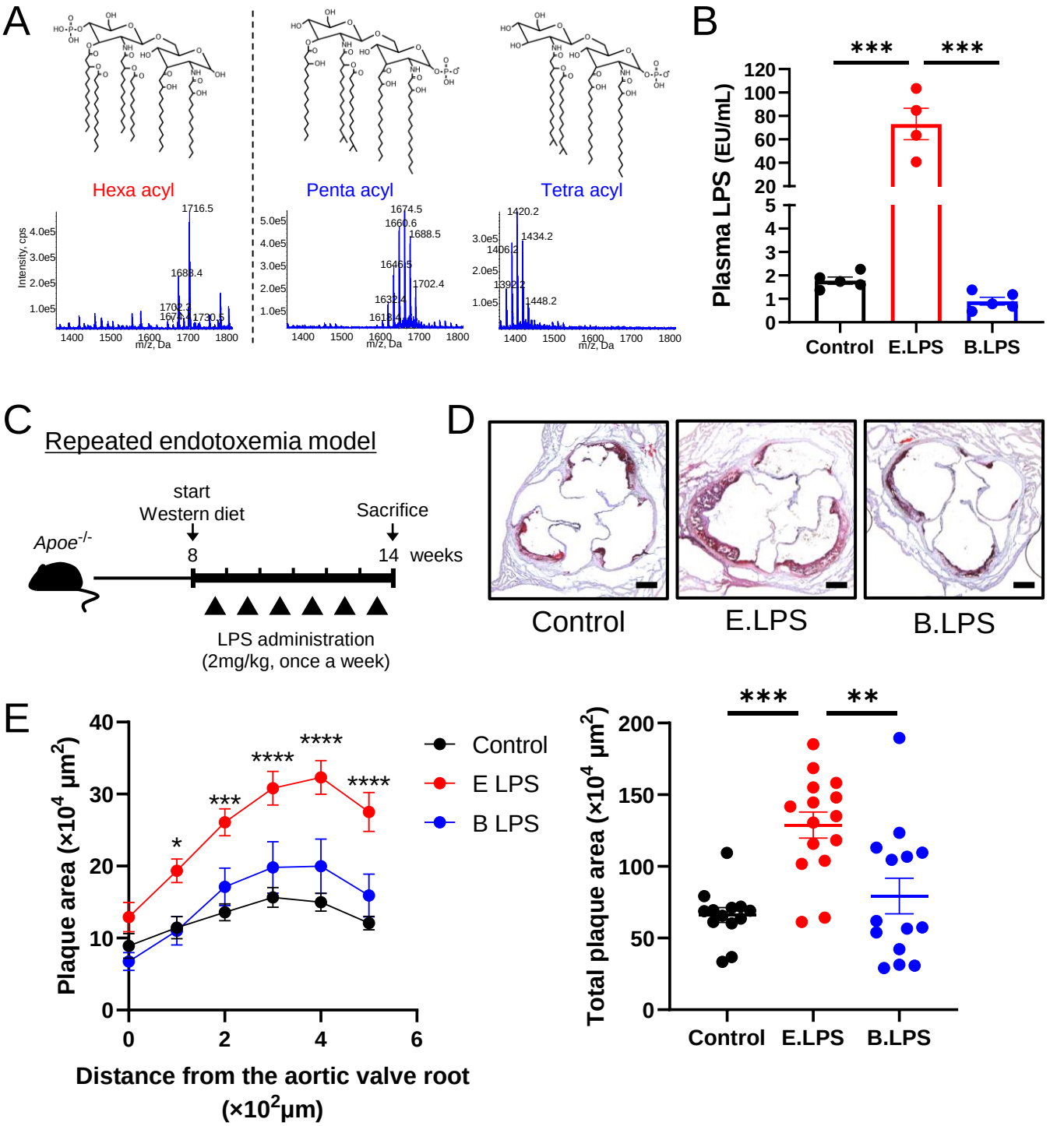


**Figure 1. Structural differences in LPS determine atherosclerotic progression in a murine model.**

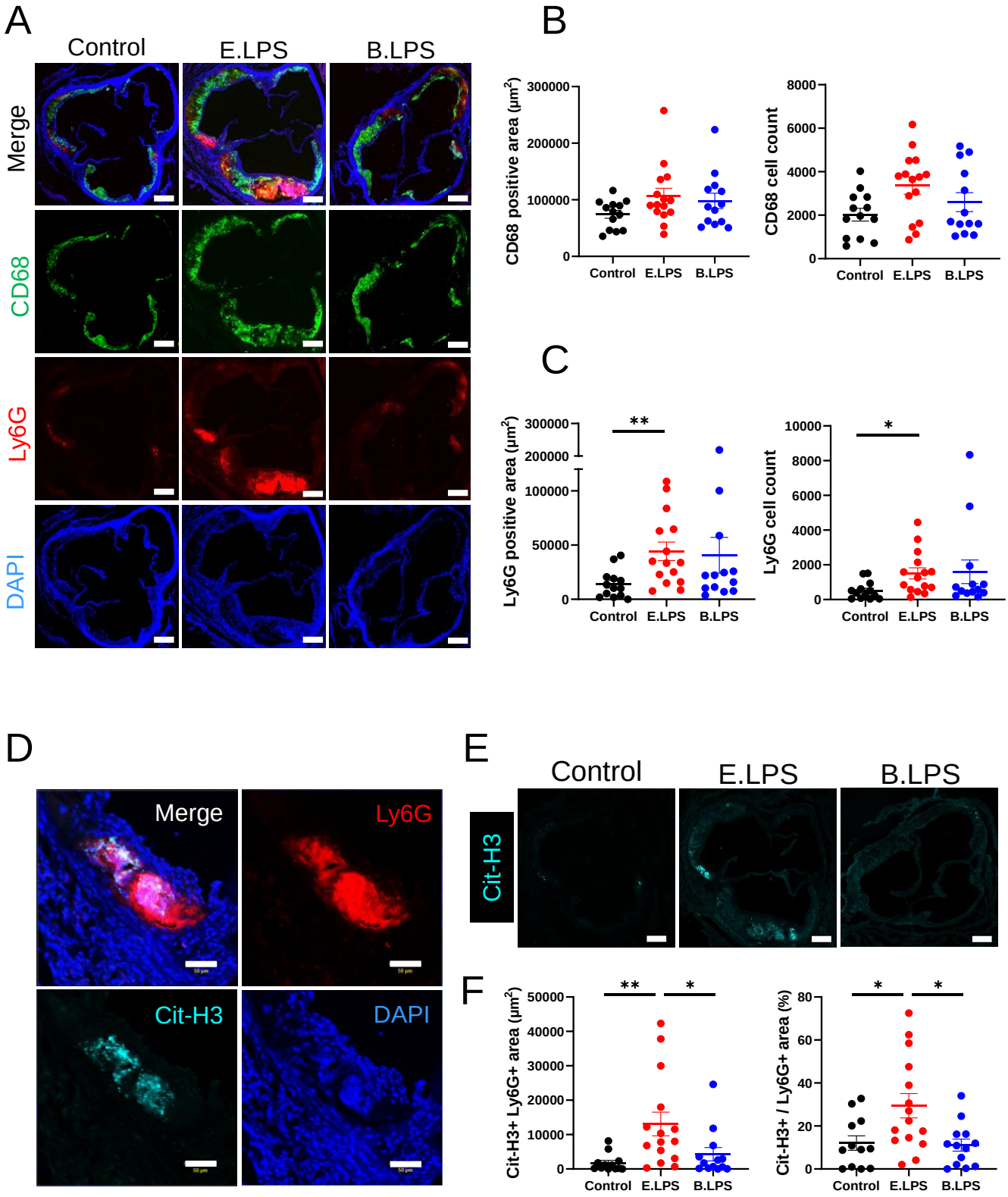


**Figure 2. *E. coli* LPS demonstrates a high ability to induce NET formation in plaque lesions.**

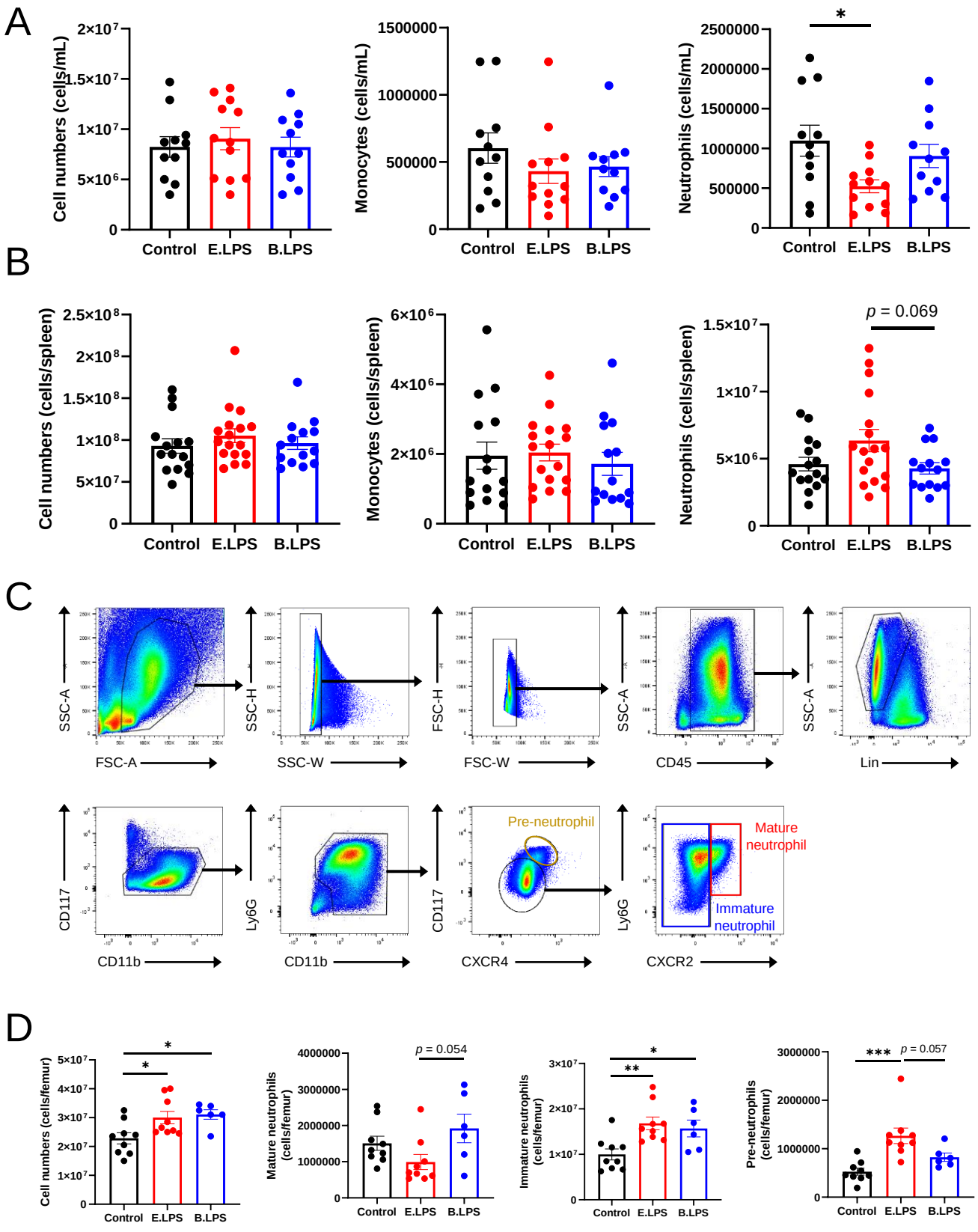


**Figure 3. Stimulation with *E. coli* LPS increases the number of neutrophil progenitor cells in the bone marrow.**

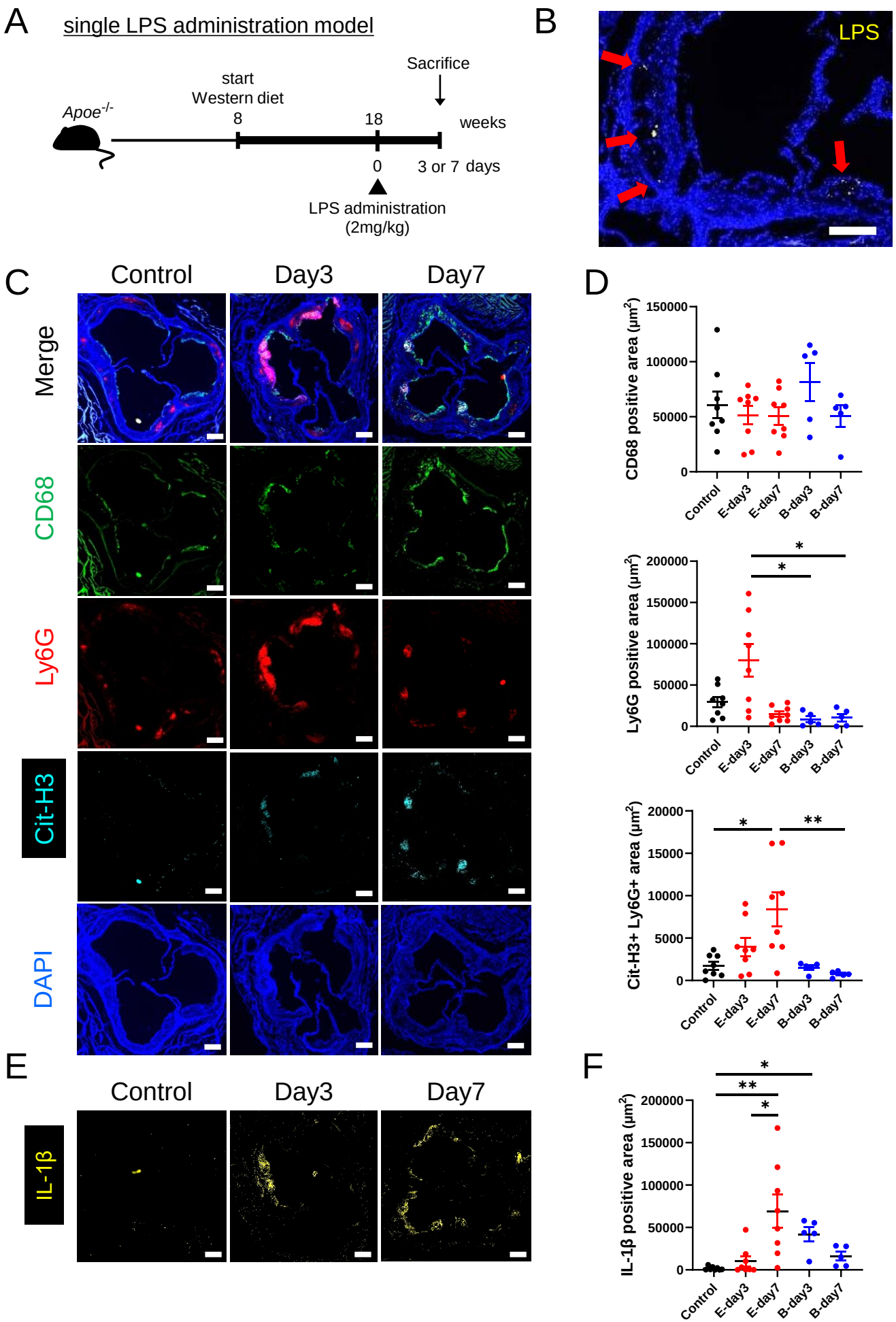


**Figure 4. Endotoxemia induces neutrophil accumulation and subsequent NET formation in plaque lesions.**

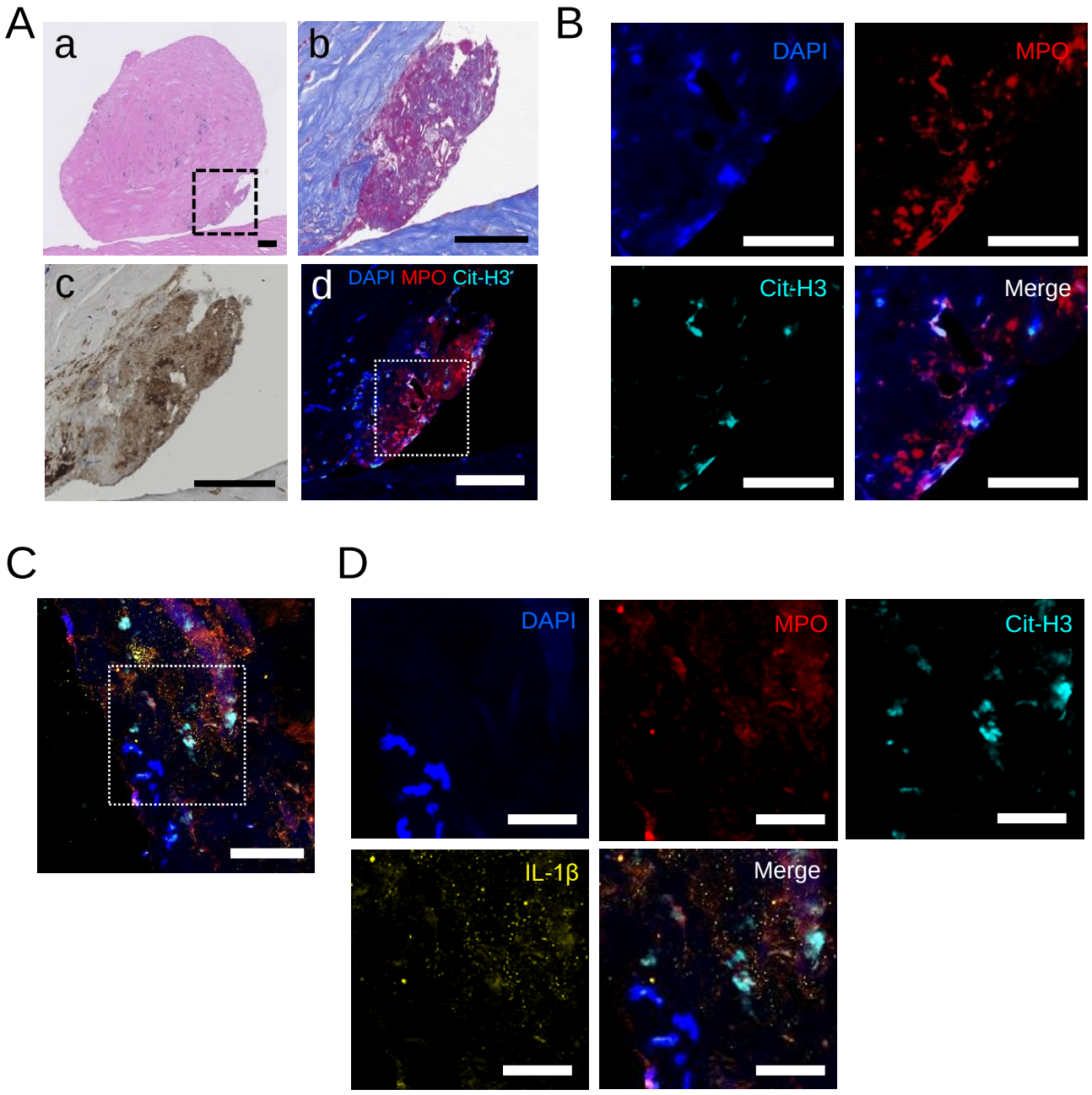


**Figure 5. NET formation and IL-1β production are observed in human coronary plaques.**